CONTRIBUTION FROM THE DEPARTMENT OF CHEMISTRY AND MATERIALS RESEARCH CENTER, NORTHWESTERN UNIVERSITY, EVANSTON, ILLINOIS 60201

# Vibrational Spectra, Vibrational Analysis, and Bonding in Acetonitrile–Boron Trifluoride

BY B. SWANSON[1] AND D. F. SHRIVER[2]

*Received December 8, 1969*

Infrared and Raman data in the 4000–70-cm$^{-1}$ region have been determined at −196° for five isotopic species of $F_3BNCCH_3$. Also, vibrational data were obtained for 3% $F_3BNCCH_3$ in host crystals of $F_3BNCCD_3$. Several interesting temperature- and host-dependent features were observed. The foregoing in conjunction with Raman polarization data for the complex in solution form the basis of assignments. Normal-coordinate calculations based on a constrained general-valence force field aid in assigning the low-frequency region. The frequencies and force constants are discussed in terms of donor–acceptor interaction.

## Introduction

Vibrational analysis provides a powerful means of elucidating donor–acceptor interaction through a comparison of frequencies and force constants for the complex with those of the free acid and base. The present study centers on boron trifluoride–acetonitrile, which is one of the few highly symmetric weak boron trifluoride complexes. While specific features of the boron trifluoride–acetonitrile spectrum have been observed and discussed,[3–6] a thorough vibrational study has not been reported previously.

## Experimental Section

**Infrared Spectra.**—The far-infrared spectra (450–50 cm$^{-1}$) were recorded on a Beckman IR-11. Calibration of the instrument was occasionally checked with atmospheric water bands and the instrument was found to be within ±0.5 cm$^{-1}$ of the recorded band positions.[7] The infrared spectra from 400 to 4000 cm$^{-1}$ were recorded on a Beckman IR-9, and the calibration was checked with $CO_2$ bands. The instrument was found to be within ±0.8 cm$^{-1}$ of the reported band positions.[7] The spectra were collected using a Wagner–Hornig type low-temperature infrared cell[8] fitted with polyethylene plates for the far-infrared region and fitted with KBr plates for the 4000–400-cm$^{-1}$ region.

Owing to the hygroscopic nature of the adducts, all sample preparations were carried out on a chemical vacuum line.[9] The adduct was sublimed onto the cold plate at −196° and the spectrum was taken while the sample was in its unannealed state. The sample was then allowed to anneal at $0° > T > -78°$ before recooling and taking the spectrum. Finally the annealed sample was warmed to −78° and the spectrum was retaken. The adduct was found to react slowly at room temperature with alkali halide window materials. Infrared spectra of the adduct which had decomposed on a KBr plate showed a broad, strong band at *ca.* 1100 cm$^{-1}$, indicating that the reaction product contains $BF_3Br^-$, $BF_4^-$, or similar species. Therefore, care was taken during the annealing process by avoiding temperatures above *ca.* 0° and clean plates were used for each run. We were unable to obtain far-infrared spectra of the annealed sample at −78° owing to inefficient thermal contact of the polyethylene cold plate with the copper block (the sample was heated by the beam and eventually sublimed onto the copper block).

**Raman Spectra.**—The Raman data were collected using a Spex 1400-II double monochromator with photon-counting detection.[10] The solid-state spectra were gathered using a 6328-Å He–Ne laser while the solution spectrum of the $^{11}B$ adduct in acetonitrile was taken using an Ar ion laser (Coherent Radiation Model 52) at 5145 Å. All peak positions were corrected to the true displacement from the exciting line using the observed exciting line position.

The solid-state Raman data were collected using a simple Raman cold cell designed for right angle viewing.[11] The sample was sublimed onto the cold finger at −196° and allowed to anneal at room temperature for 0.5 hr before recooling and taking the spectrum.

The Raman spectrum of the normal isotopic adduct was taken in both acetonitrile and nitromethane solutions. A drawing of the solution cell is presented in Figure 1 and is largely self-explanatory. The cell consists of a Pyrex Raman liquid cell and a reaction tube separated by a fine frit. Teflon-in-glass needle valves on either side of the frit enable all manipulations to be performed on a chemical vacuum line. After formation of the adduct in the previously evacuated reaction tube, solvent was distilled onto the adduct, and the solution was filtered through the frit by application of dry nitrogen pressure. Depolarization ratios were calculated from consecutive scans of the peak, first with the incident beam polarized in the parallel orientation and the analyzer parallel, $Z(Y,Y)X$, and then with the incident beam parallel and the analyzer perpendicular, $Z(Y,Z)X$.[12] Peak areas were used in the calculation for all bands except two which are on the wings of a solvent peak and required the use of peak heights. No corrections were made for convergence error.

## Assignments

Unless otherwise specified, all spectra reported in this section were gathered at −196° on annealed solids. Assignments are primarily based on the $C_{3v}$ symmetry which is the presumed geometry of the isolated molecule. For this symmetry seven $A_1$ modes and eight E modes are Raman and infrared active while one $A_2$ mode is totally inactive. Certain features of the spectra are explained in terms of selection rules for the solid state. The adduct crystallizes in the centrosymmetric space group Pnma with four molecules per unit cell at sites of $C_s$ symmetry.[13] The centric space group requires the

(1) NDEA Fellow, 1968–1970.
(2) Alfred P. Sloan Fellow; addressee for correspondence.
(3) H. J. Coerver and C. Curran, *J. Am. Chem. Soc.*, **80**, 3522 (1958).
(4) J. Le Calvé, Doctoral Thesis, Bordeaux, 1966.
(5) K. F. Purcell and R. S. Drago, *J. Am. Chem. Soc.*, **88**, 919 (1966).
(6) I. R. Beattie and T. Gilson, *J. Chem. Soc.*, 2292 (1964).
(7) K. N. Rao, C. J. Humphreys, and D. H. Rank, "Wavelength Standards in the Infrared," Academic Press, New York, N. Y., 1966, p 145.
(8) (a) E. L. Wagner and D. F. Hornig, *J. Chem. Phys.*, **18**, 296 (1950); (b) D. F. Shriver, "Manipulation of Air Sensitive Compounds," McGraw-Hill Book Co., Inc., New York, N. Y., 1969, p 95.
(9) Reference 8b, Chapter 1.
(10) I. Wharf and D. F. Shriver, *Inorg. Chem.*, **8**, 914 (1969).
(11) D. F. Shriver, B. Swanson, and N. Nelson, *Appl. Spectry.*, **23**, 274 (1969).
(12) The notation is that of T. C. Damen, S. P. S. Porto, and B. Tell, *Phys. Rev.*, **142**, 570 (1966).
(13) B. Swanson, D. F. Shriver, and J. A. Ibers, *Inorg. Chem.*, **8**, 2182 (1969).

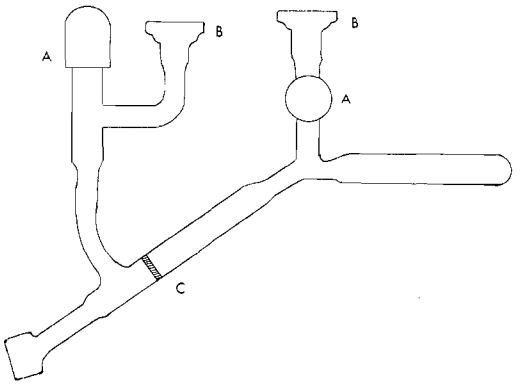


Figure 1.—Raman liquid cell: A, 4-mm Teflon-in-glass needle valves; B, 18/9 O-ring joints; C, 10-mm fine frit; windows on the cell are parallel Pyrex flats fused to 10-mm Pyrex tubing (lower left of figure).

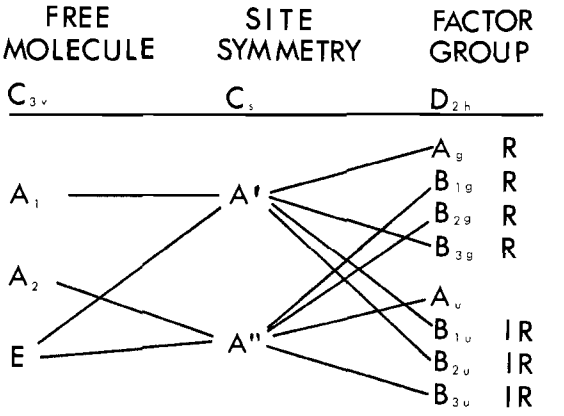


Figure 2.—Correlation table for $F_3BNCCH_3$.

mutual exclusion selection rule of infrared- and Raman-active modes. Figure 2 contains a correlation diagram relating symmetry species of the isolated molecule ($C_{3v}$) with those of the site symmetry ($C_s$) and the factor group ($D_{2h}$). Selection rules derived from a permutation group treatment are described later. These may explain the lack of observable E symmetry $CH_3$ rock and stretch modes in the Raman spectrum.

The designation of fundamentals is given in Table I for the isolated molecule. In the following discussion, data on the normal isotopic molecule are given without comment, while special isotopic substitution is designated by listing only the enriched isotope, *e.g.*, $^{10}BD = F_3{}^{10}BNCCD_3$.

**4000–2000 Cm$^{-1}$.**—This region contains $\nu_1$ ($A_1$, $CH_3$ stretch), $\nu_9$ (E, $CH_3$ stretch), and $\nu_2$ ($A_1$, C≡N stretch) fundamentals and the assignments present no difficulty. The fundamental $\nu_1$, which is observed at *ca.* 2956 cm$^{-1}$ for the H isotopic species and at *ca.* 2122 cm$^{-1}$ for the deuterated species, is a medium band in the infrared spectra and very strong in the Raman spectra (Figure 3). The $\nu_9$ vibration appears with weak intensity in

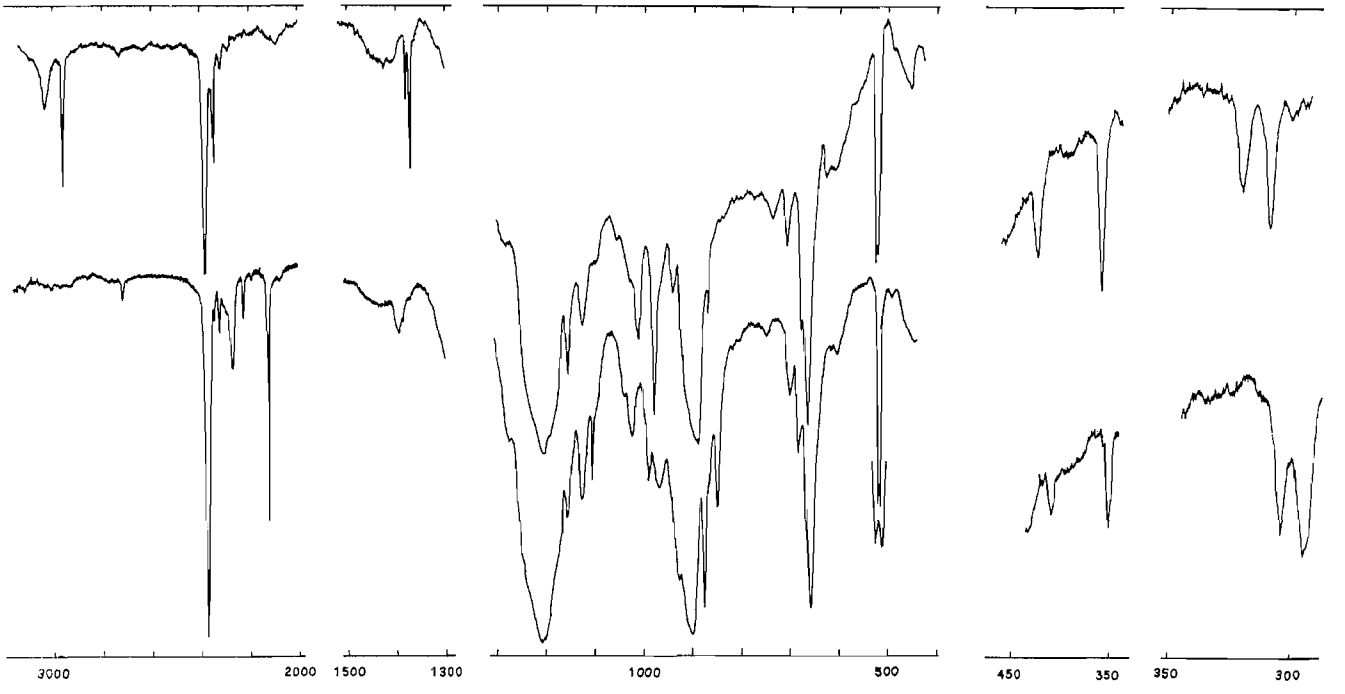


Figure 3.—Infrared spectra of $F_3{}^{10}BNCCH_3$ and $F_3{}^{10}BNCCD_3$ (cm$^{-1}$). The upper graph is the spectrum of $F_3{}^{10}BNCCH_3$ and the lower graph of $F_3{}^{10}BNCCD_3$ in all regions. The region below 450 cm$^{-1}$ was scanned with the Beckman IR-11, and both spectra were taken using annealed samples at *ca.* −196°.

TABLE I
DESCRIPTION AND NUMBERING OF THE FUNDAMENTAL VIBRATIONS OF $F_3BNCCH_3$

| | | | | | | | |
|---|---|---|---|---|---|---|---|
| $A_1$ class | | | | E class | | | |
| $\nu_1$ | sym | $CH_3$ | str | $\nu_9$ | asym | $CH_3$ | str |
| $\nu_2$ | sym | C≡N | str | $\nu_{10}$ | asym | $CH_3$ | def |
| $\nu_3$ | sym | $CH_3$ | def | $\nu_{11}$ | asym | $BF_3$ | str |
| $\nu_4$ | sym | C—C | str | $\nu_{12}$ | asym | $CH_3$ | rock |
| $\nu_5$ | sym | $BF_3$ | str | $\nu_{13}$ | asym | $BF_3$ | def |
| $\nu_6$ | sym | B—N | str | $\nu_{14}$ | asym | NCC | def |
| $\nu_7$ | sym | $BF_3$ | def | $\nu_{15}$ | asym | $BF_3$ | rock |
| | | | | $\nu_{16}$ | asym | BNC | def |
| $A_2$ class | | | | | | | |
| $\nu_8$ | torsion | | | | | | |

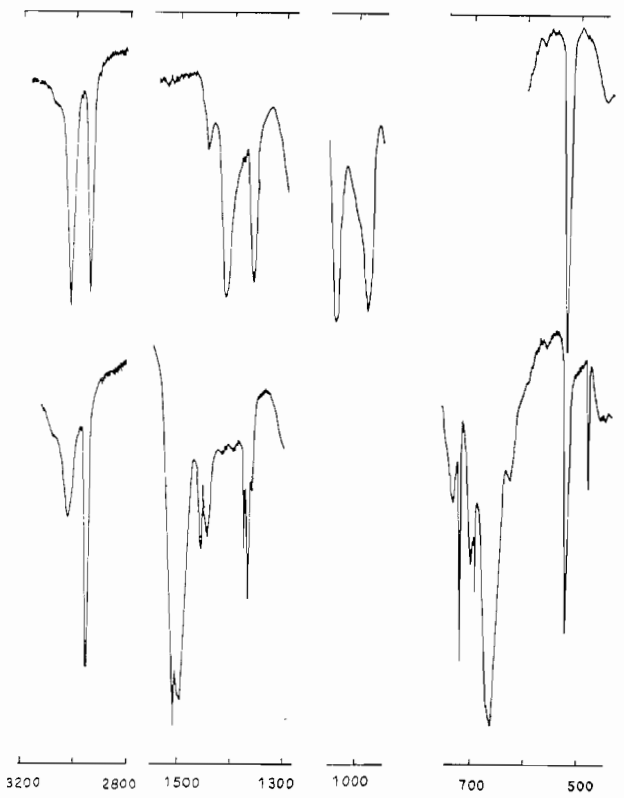


Figure 4.—Temperature and phase dependence of the infrared spectrum of $F_3{}^{10}BNCCH_3$. The upper spectrum is that of an unannealed sample at −196° and the lower represents an annealed sample at −78°. Compare with annealed spectra obtained at −196° in Figure 3.

the infrared spectra and is not present in the Raman spectra for the H isotopic species but appears as a weak band in the Raman spectra of the deuterated molecules (*ca.* 3025 $cm^{-1}$ for H molecules and *ca.* 2270 $cm^{-1}$ for the deuterated molecules). The fundamentals $\nu_1$ and $\nu_9$ for all isotopic molecules are close to the values found for free acetonitrile.[14] The vibration $\nu_2$ is very strong in both the Raman and the infrared spectra and occurs *ca.* 100 $cm^{-1}$ higher than the parent acetonitrile. Raman spectra of the $^{11}B$ isotopic molecule in acetonitrile solution showed $\nu_2$ to be polarized—$\rho_s = 0.16$.

Spectra of unannealed samples show an intensity enhancement of $\nu_9$ for the H isotopic species in the infrared spectra (Figure 4). This phenomenon is observed for all modes associated with the methyl portion of the H isotopic molecule and is less noticeable for modes associated with $CD_3$.

A number of fairly prominent features may be attributed to overtones and combination bands. The Raman spectra of the deuterated molecules exhibit peaks around 2225 $cm^{-1}$ which are absent in the infrared spectra. A reasonable assignment for these peaks is $2\nu_3$ ($A_1$, $CD_3$ deformation). The H isotopic molecules show a satellite peak of medium intensity to the low-frequency side (2340 $cm^{-1}$) of the C≡N stretch, which may be attributed to the combination band $\nu_3 + \nu_4$ ($A_1$, $CH_3$ deformation and C—C stretch, respectively)

(14) F. W. Parker, A. H. Nielson, and W. H. Fletcher, *J. Mol. Spectry.*, **1**, 107 (1957); W. H. Fletcher and C. S. Shoup, *ibid.*, **10**, 300 (1963); B. Swanson and D. F. Shriver, unpublished spectra of the liquid.

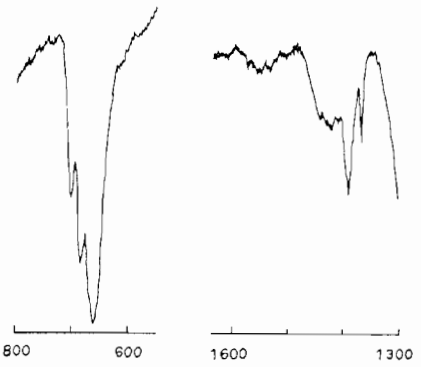


Figure 5.—Infrared spectrum of 3% $F_3{}^{10}BNCCH_3$ in host crystals of $F_3{}^{10}BNCCD_3$ at −78°.

in Fermi resonance with $\nu_2$. In agreement with this interpretation the satellite is virtually absent in the deuterated molecule and is *ca.* 20 $cm^{-1}$ lower in the $^{15}N$ isotopic molecule ($\nu_4$ is decreased by 10 $cm^{-1}$ for the $^{15}N$ species). In the $^{15}N$ isotopic molecule where the separation of $\nu_2$ and the combination band is reduced, the intensity of the satellite is nearly equal to that of $\nu_2$. Remaining bands in this region are very weak and possible assignments are presented in Tables II and III.

**2000–1300 $cm^{-1}$.**—This region contains $\nu_3$ ($A_1$, $CH_3$ deformation) and $\nu_{10}$ (E, $CH_3$ deformation) for the H isotopic molecules and presents no problem in assignments. In the infrared spectra $\nu_3$ appears as a sharp doublet at *ca.* 1372 $cm^{-1}$ (Figure 3) and in the Raman spectra as a singlet. This frequency compares favorably with that of the $CH_3$ deformation in free acetonitrile, 1389 $cm^{-1}$.[14] The splitting disappears for the $^{10}B$ isotopic molecule when it is present in 3% concentration in a lattice of the $^{10}BD$ molecule (Figure 5), which indicates that the splitting is caused by intermolecular coupling. The assignment of both peaks to $\nu_3$ is also supported by a similar splitting in the infrared spectra of the $^{10}B$ and $^{11}B$ boron trichloride adducts of acetonitrile (Swanson and Shriver, unpublished work). While the factor group analysis (Figure 2) predicts two active Raman modes as well as two active infrared modes, only one peak is observed in the Raman spectra which may be due to lack of resolution in the Raman spectra. The splitting of $\nu_3$ in the infrared spectra appears only upon annealing the sample (Figures 3 and 4).

The $\nu_{10}$ infrared absorption is assigned to a strong peak at 1430 $cm^{-1}$ in the unannealed sample which loses intensity and broadens upon annealing (Figures 3 and 4). This is 20 $cm^{-1}$ lower than the corresponding band in acetonitrile. A striking feature of the 1400–1500 $cm^{-1}$ region is the appearance of two very strong doublets at *ca.* 1450 and *ca.* 1500 $cm^{-1}$ upon warming the sample. These bands will be discussed later. The remaining bands in this region are quite weak and can be assigned to various combination bands or overtones (Table II).

**1300–1100 $cm^{-1}$.**—This region is dominated in the infrared spectra by a strong band at *ca.* 1200 $cm^{-1}$ (Figure 3) which can be attributed to $\nu_{11}$ (E, $BF_3$

TABLE II

OBSERVED INFRARED FREQUENCIES ($cm^{-1}$)[a]

| $F_3BNCCH_3$ | $F_3BNCCD_3$ | $F_3B^{15}NCCH_3$ | $F_3{}^{10}BNCCH_3$ | $F_3{}^{10}BNCCD_3$ | Assignments |
|---|---|---|---|---|---|
| ... | ~130 vs, br | ~130 vs, br | ... | ... | ? |
| 308.9 m | 294 ms | 307.5 m | 308.4 m | 293.4 s | $\nu_{15}$ |
| 319.7 w | 303.3 ms | 318.1 w | 319.5 w | 302.8 ms | |
| 359.2 s | 348.7 s | 356.1 s | 358.6 s | 347.8 ms | $\nu_7$ |
| 422.8 mw | 407 m | 417.7 mw | 422.2 mw | 406.5 mw | $\nu_{14}$ |
| ~450 vvw | 453.4 w | ... | 453 w | 450 vw | ? |
| ~490 vvw | ... | ... | ~490 vvw | 494 vvw | ? |
| 519.0 m | 516.2 s | 514.3 m | 520.4 ms | 517.4 ms | $\nu_{13}$ |
| 522.6 m | 521.5 s | 517.7 m | 523.7 ms | 520.5 ms | |
| ~610 w | 604 vw | | ~615 vw | 601 vw | $2\nu_{15}$ |
| 657.1 s | 650.5 vs | 654.6 s | 661.2 vs | 656.7 vs | $\nu_6$ |
| 675 m | 666.6 s, sh | 673.4 m | 676.7 sh | 668.2 sh | $\nu_7 + \nu_{15}$ |
| 706.3 w | 684.3 m | 701.6 w | 705.2 w | 684.1 sh | $2\nu_7$ |
| ~730 vw | 701.4 mw | ... | ~720 vw | 700.8 mw | $\nu_{14} + \nu_{15}$ |
| ... | ... | ... | ... | 746.5 vw | $\nu_7 + \nu_{14}$ |
| ... | 848.0 s | ... | ... | 850.1 ms | $\nu_{12}$ |
| 883.5 s | 873.5 vs | 879.0 vs | 867.7 m | 878.5 vs | $\nu_5$ and $\nu_4$ (D) |
| 904.4 s | 890.8 vvs | 900.4 s | 893.1 vvs | 904.8 vvs | |
| ... | 907.3 sh | ... | ... | ... | ? |
| ~938 w | 926.8 m, sh | ~932 vw | 939.6 w | 930.2 sh | $\nu_{13} + \nu_{14}$ |
| ... | 947.7 vw | ... | ... | 948.2 w, sh | $\nu_6 + \nu_{15}$ |
| 978.7 m | ... | 968.7 s | 979.0 s | ... | $\nu_4$ |
| ... | 982 m | ... | ... | 970.2 m | $\nu_1 - \nu_3$ |
| 1004.0 w | ... | 999.0 w | 1012.2 m | 992.0 m | $\nu_6 + \nu_7$ |
| 1031.3 w | ... | ~1032 w | 1028.6 w | ... | $\nu_{12}$ |
| ... | 1024.7 m, br | ... | ... | 1025.7 mw | $\nu_{10}$ |
| ~1050 vvw | ... | ... | ~1057 vvw | 1042.1 sh | $2\nu_{13}$ |
| ... | 1106.7 m | ... | ... | 1106.6 m | $\nu_3$ |
| 1127.4 mw | 1129.1 sh | 1126.3 m | 1126.6 m | 1127.4 m | $\nu_6 + \nu_7$ |
| 1157.2 vs | ... | 1156.1 vvs | 1157.3 ms | 1156.4 m | $\nu_6 + \nu_{13}$ |
| 1188.4 s, sh | 1170 vvs, br | 1182.6 sh | ~1183 sh | 1187.4 sh | $\nu_{11}$ |
| 1208.4 s | 1216 vs | 1204 m | 1205.8 vvs | 1206.8 vvs | |
| ... | ... | ... | ~1237 sh | 1235.2 sh | $\nu_7 + \nu_5$ |
| ~1285 vw | 1267 w, sh | 1288 w | ~1290 vvw | 1276 w, br | ? |
| 1369.6 mw | ... | 1369.2 m | 1370 m | ... | $\nu_3$ |
| 1374.4 mw | ... | 1377.5 m | 1378.4 w | ... | |
| 1385.4 vvw | 1385.2 w | ... | ... | 1395.4 w | $\nu_5 + \nu_{13}$ |
| ~1430 w, br | ... | ~1417 vw | ~1430 w | ... | $\nu_{10}$ |
| ... | 1428.9 w, br | ... | ... | ~1425 vw, sh | $\nu_4 + \nu_{13}$ |
| ... | 1952.1 vw | ... | ... | ... | $\nu_3 + \nu_4$ |
| ... | 2018 w | ... | ~2090 vw | ~2070 vvw | ? |
| ... | 2123.5 ms | ... | ... | 2121.9 ms | $\nu_1$ |
| ... | 2190 vvw | ... | ... | ... | ? |
| ... | 2223.5 w | ... | ... | 2223.4 w | $2\nu_3$ |
| ... | 2271 mw | ... | ... | 2269 mw | $\nu_9$ |
| ... | 2290.5 w | ... | ... | ... | ? |
| 2312.0 vw | 2320.5 vw | ... | ~2320 vw | 2320 w | ? |
| 2340.0 mw | 2342 vvw | 2324.6 s | 2340.4 m | 2340 vvw | $\nu_3 + \nu_4$ |
| 2376.2 s | 2373 vs | 2349.2 s | 2373.9 s | 2373.8 vs | $\nu_2$ |
| ... | 2714 w | ... | ... | 2710 vvw | $\nu_9 + \nu_{14}$ |
| | | | | | $\nu_9 + \nu_{13}$ |
| 2956.0 m | ... | 2955.9 m | 2957.0 m | ... | $\nu_1$ |
| 3029.5 w | ... | 3026 w | 3029.0 mw | ... | $\nu_9$ |
| ... | ... | ... | ... | 3251 vvw | $\nu_1 + \nu_3$ |
| ... | 3481 w | ... | ... | ~3475 w | $\nu_2 + \nu_{10}$ |

[a] These data represent spectra of annealed polycrystalline samples at *ca.* −196°.

stretch). No peaks are found in the Raman spectra except $\nu_3$ ($A_1$, $CD_3$ deformation) at 1106 $cm^{-1}$ which is present in the infrared spectra as a sharp singlet (Figure 3). Structure in the 1200-$cm^{-1}$ band includes an unusually strong feature at *ca.* 1157 $cm^{-1}$, a strong shoulder at *ca.* 1188 $cm^{-1}$, and a strong peak at *ca.* 1210 $cm^{-1}$ for the normal and $^{15}N$ isotopic molecules. In addition the D isotopic molecule exhibits a very strong, broad peak at *ca.* 1170 $cm^{-1}$ and another strong peak at 1216 $cm^{-1}$. In the relatively uncluttered spectra of the $^{10}B$ and $^{10}BD$ isotopic species, $\nu_{11}$ can be assigned to the broad band at *ca.* 1208 $cm^{-1}$. For the more complex spectra of the normal and $^{15}N$ isotopic molecules it is thought that the sharp 1157-$cm^{-1}$ band and the strong shoulder at 1188 $cm^{-1}$ obscure the maximum for $\nu_{11}$. The value of $\nu_{11}$ for all $^{11}B$ isotopic molecules is thought to be close to that found for the D molecule, 1170 $cm^{-1}$. The feature which appears in the normal

TABLE III

OBSERVED RAMAN FREQUENCIES ($cm^{-1}$)[a]

| $F_3BNCCH_3$ | | $F_3BNCCD_3$ | $F_3{}^{10}BNCCH_3$ | $F_3{}^{10}BNCCD_3$ | Assignment |
|---|---|---|---|---|---|
| 98.5 m | ... | 97.3 m | 100.0 m | 98.0 m | $\nu_{16}$ |
| 129.6 vs | ... | 124.7 s | 138.9 vs | 127.1 s | ? |
| 309.0 w | 0.8[b] | 304.1 m | 310 vw | 302.3 m | $\nu_{15}$ |
| 361.4 m | *Ca.* 0[b] | 344 s | 356.4 m | 343.0 m | $\nu_7$ |
| 418.2 s | 0.75[b] | 403.5 vs | 421.0 s | 402.4 s | $\nu_{14}$ |
| 526.6 m | 0.75[b] | 525.4 m | 530.2 m | 524.6 m | $\nu_{13}$ |
| 645.8 w | *Ca.* 0[b] | 644.3 mw | 659.7 w | 654.8 m | $\nu_6$ |
| 855.5 s | *Ca.* 0[b] | 857.2 vs | 874.6 m | 868.5 mw | $\nu_5$ |
| 971.1 m | *Ca.* 0[b] | 892.2 m | 982.9 w | 899.8 mw | $\nu_4$ |
| 1037.6 w[c] | 0.76[b] | ... | ... | ... | $\nu_{12}$ |
| 1372.2 s | 0.36[b] | 1112.4 m | 1373.7 m | 1111.5 mw | $\nu_3$ |
| ... | ... | 2122.3 vvs | ... | 2124.3 vvs | $\nu_1$ (D) |
| ... | ... | 2225.9 m | ... | 2224.9 m | $2\nu_8$ |
| ... | ... | 2271.8 m | ... | 2271.8 m | $\nu_9$ (D) |
| 2372.8 vs | ... | 2371.5 vvs | 2376.8 vs | 2372.9 vs | $\nu_2$ |
| ... | ... | 2375.3 w, sh | ... | 2375.7 w, sh | $\nu_3 + \nu_4 + \nu_7$ |
| 2953.8 vs | ... | ... | 2955.9 s | ... | $\nu_1$ (H) |

[a] Observed Raman frequencies from annealed solid samples of $F_3BNCCH_3$ at $-196°$. [b] Depolarization ratios found for $F_3BNCCH_3$ in acetonitrile solution. A value of 0.75 corresponds to a totally depolarized band. [c] Frequency obtained from solution spectrum and not observed in solid-state spectrum.

isotopic molecules at 1208 $cm^{-1}$ can be attributed to the $\nu_{11}$ for the $^{10}B$ isotopic species (20% $^{10}B$ and 80% $^{11}B$). The strong band at 1157 $cm^{-1}$ may be a combination of $\nu_6 + \nu_{13}$, rendered intense by Fermi resonance with $\nu_{11}$. The weak shoulders at *ca.* 1285 and *ca.* 1237 $cm^{-1}$ ($^{10}B$ species only) can be assigned to $2\nu_6$ ($A_1$, B–N stretch) and $\nu_5 + \nu_7$ ($A_1$, $BF_3$ stretch, and $A_1$, $BF_3$ deformation, respectively).

An alternate set of assignments for $\nu_{11}$ is 1157 $cm^{-1}$ for the normal and $^{11}B^{15}N$ isotopic molecules and 1170 $cm^{-1}$ for the D molecule. This explanation results in an unlikely shift of 13 $cm^{-1}$ between normal and D isotopic species. A third explanation of this region is that, owing to factor group splitting, all three bands (*ca.* 1208, *ca.* 1188, and *ca.* 1157 $cm^{-1}$) can be assigned to $\nu_{11}$. This is unlikely since no isotopic effects are observed for these bands between $^{10}B$ and $^{11}B$ species.

**1100–930 $Cm^{-1}$.**—This region contains $\nu_4$ ($A_1$, C–C stretch) and $\nu_{10}$ (E, $CD_3$ deformation) for the D isotopic species. The peak at *ca.* 1030 $cm^{-1}$ for the H molecules (Figures 3 and 4) is assigned to $\nu_{12}$ because it shows an increase in intensity for the unannealed sample and is similar in frequency to the $CH_3$ rock mode of free acetonitrile (1040 $cm^{-1}$).[14] This assignment is verified by the solution Raman spectrum of the normal isotopic adduct in acetonitrile which exhibits a depolarized band at 1035 $cm^{-1}$ (Figure 6, $\rho_s = 0.76$), which can be attributed to the adduct since there is negligible interference from the extremely weak $CH_3$ rock of the acetonitrile solvent. The strong band at *ca.* 979 $cm^{-1}$ in the infrared spectra of the H molecules (Figure 3) can be assigned to $\nu_4$. This represents a 60-$cm^{-1}$ increase over the corresponding frequency for free acetonitrile. The only band which is comparable to the corresponding frequency for the free acetonitrile is the weak peak at *ca.* 940 $cm^{-1}$ which can be assigned to the combination $\nu_{12} + \nu_{15}$. A Raman peak for the $^{10}B$ isotopic molecule at *ca.* 983 $cm^{-1}$ and the presence of a polarized band at 972 $cm^{-1}$ ($\rho_s = 0.0$) in the solution spectrum of the $^{11}B$ adduct in acetonitrile confirms the assignment of the higher and more intense peak at *ca.* 979 $cm^{-1}$ to $\nu_4$. This assignment is also supported by a *ca.* 10-$cm^{-1}$ decrease observed for the $^{11}B^{15}N$ molecule. (A corresponding decrease in the C–C stretch is noted for free acetonitrile.)

The $\nu_{10}$ fundamental for the deuterated molecules can be assigned easily to the peaks at *ca.* 1025 $cm^{-1}$. This position is close to that of the corresponding vibration in free acetonitrile (1046 $cm^{-1}$)[14] and is reasonable on the basis of the enhancement of intensity which is observed for the unannealed sample. The remaining bands are weak and possible assignments are given in Tables II and III.

**930–750 $Cm^{-1}$.**—This portion of the spectrum contains $\nu_5$ ($A_1$, $BF_3$ stretch) for all isotopic molecules and $\nu_4$ ($A_1$, C–C stretch) and $\nu_{12}$ (E, $CD_3$ rock) for the deuterated species. The infrared spectra are complicated so positions of the fundamentals are most easily found in the Raman spectra where peaks are observed at 855.5 and 874.6 $cm^{-1}$ for the normal and $^{10}B$ molecules, respectively. The deuterated molecules have bands at *ca.* 860 and *ca.* 895 $cm^{-1}$. Also, the Raman spectrum of the $^{11}B$ molecule in acetonitrile solution (Figure 6) shows the 855.5-$cm^{-1}$ band to be polarized ($\rho_s \approx 0$). The bands at 892.2 and 899.8 $cm^{-1}$ for the $^{11}BD$ and $^{10}BD$ isotopic molecules, respectively, can be assigned to $\nu_4$, and the remaining peaks can be assigned to $\nu_5$. The $^{11}B$, $^{10}B$ isotopic shifts for $\nu_5$ of 20 $cm^{-1}$ are reasonable, and, as is found for the H isotopic species, $\nu_4$ has been shifted ~60 $cm^{-1}$ to a higher frequency when compared to free deuterioacetonitrile.[14] The relative shifts of $\nu_4$ and $\nu_5$ upon isotope substitution are correctly predicted by the normal-coordinate analysis (see below).

The infrared spectra of both deuterated molecules also exhibit a sharp band at *ca.* 850 $cm^{-1}$ which can be assigned to $\nu_{12}$ (E, $CD_3$ rock). This band does not appear in spectra of the H molecules and the value agrees quite well with the corresponding vibration in

free deuterioacetonitrile.[14] The remaining portions of the infrared spectra are not as easily explained. It is obvious from comparison of Raman and infrared spectra that $\nu_5$ does not coincide in both techniques. For example the infrared spectrum of the normal isotopic molecule shows strong peaks at 883.5 and 904.4 $cm^{-1}$ but no peaks at 855.5 $cm^{-1}$ where $\nu_5$ appears in the Raman spectrum. This lack of coincidence is attributed to factor group splitting.

The $^{10}B$ molecule shows a very strong band at 893.1 $cm^{-1}$ which can be assigned to $\nu_5$ (the only other band in this region is a medium-intensity peak at 867.7 $cm^{-1}$). The $^{10}BD$ molecule has a strong sharp peak at 878.5 and a very strong band at 904.8 $cm^{-1}$. If the $\nu_5$ assignment from the $^{10}B$ molecule is used as an approximation for $\nu_5$ in $^{10}BD$, then $\nu_4$ (taken from Raman assignment) and $\nu_5$ will both be found at *ca.* 890 $cm^{-1}$ in the infrared spectrum. It is felt that the strong broad band at 904.8 $cm^{-1}$ contains both $\nu_4$ and $\nu_5$ while the sharp band at 878.5 $cm^{-1}$ can be assigned to the combination $\nu_{13} + \nu_{15}$ (E, $BF_3$ deformation, and E, $BF_3$ rock, respectively).

The assignments for $\nu_5$ from the infrared data are approximate and those for $\nu_4$ are no better. Tentative assignments for the remaining isotopic molecules are presented in Table II, and the treatment of $\nu_4$ and $\nu_5$ for the normal-coordinate analysis is discussed later.

**750–600 $Cm^{-1}$.**—This region is dominated in the infrared spectra by a strong band at *ca.* 650 $cm^{-1}$ which can be assigned to $\nu_6$ ($A_1$, B–N stretch). A single band at *ca.* 650 $cm^{-1}$ is observed for all the isotopic molecules in the Raman spectra (Figure 6) and the spectrum of the normal isotopic adduct in acetonitrile solution showed this band to be polarized ($\rho_s = 0.0$). This position for B–N stretch is low when compared to boron trifluoride adducts of trimethylamine[15] and ammonia,[16] which might be expected since acetonitrile is a much weaker base than ammonia or trimethylamine.[17] The two remaining features in the spectra (*ca.* 706 and *ca.* 730 $cm^{-1}$ for the H molecules and *ca.* 685 and *ca.* 701 $cm^{-1}$ for the D molecules) can be assigned to overtones or combinations (Table II).

Upon warming to −78° two remarkably sharp spikes appear at *ca.* 718 and *ca.* 690 $cm^{-1}$ (a similar spike is observed at *ca.* 480 $cm^{-1}$). This temperature effect, which is reversible and does not appear for the deuterated molecules, is discussed later.

**600–50 $Cm^{-1}$.**—This region contains the skeletal vibrations $\nu_7$ ($A_1$, $BF_3$ deformation), $\nu_{13}$ (E, $BF_3$ deformation), $\nu_{14}$ (E, NCC linear angle deformation), $\nu_{15}$ (E, $BF_3$ rock), and $\nu_{16}$ (E, BNC linear angle deformation) as well as the inactive mode $\nu_8$ ($A_2$, torsion). The infrared spectra exhibit five bands in the region between 600 and 290 $cm^{-1}$ (Figure 3). The band at *ca.* 520 $cm^{-1}$ in the infrared spectra for samples which have not been annealed appears as a singlet. Upon annealing, however, this band appears as a sharp doublet. The bands

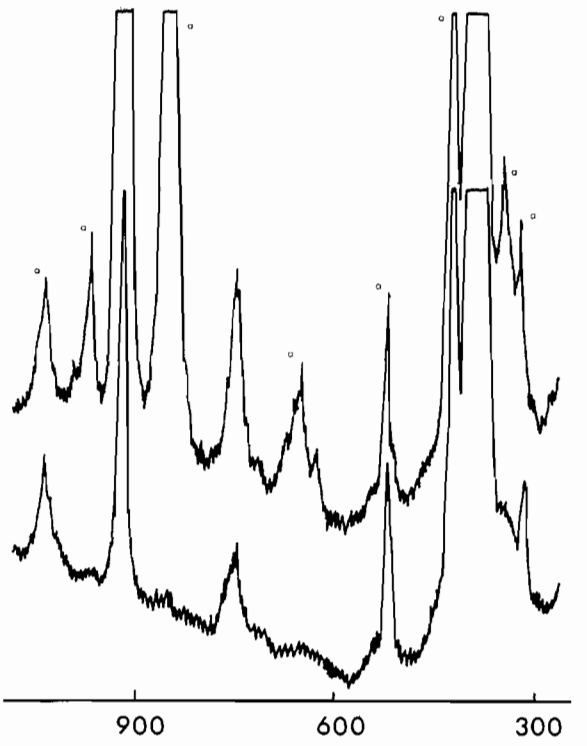


Figure 6.—Raman spectrum of $F_3BNCCH_3$ in $NCCH_3$ solution. The upper graph represents $Z(Y,Y)X$ polarization while the lower one represents $Z(Y,Z)X$. The peaks attributed to the adduct are marked.

at *ca.* 320 and *ca.* 310 $cm^{-1}$ also appear as single features in unannealed samples but can be resolved after annealing. Finally, a broad, unresolved feature is observed at *ca.* 130 $cm^{-1}$. Raman spectra for the solid exhibit only four bands in the region 600–290 $cm^{-1}$ with singlets observed at *ca.* 520 and *ca.* 310 $cm^{-1}$, rather than the doublets found in the infrared spectra. The Raman spectra also contain bands at *ca.* 130 and *ca.* 100 $cm^{-1}$.

The normal isotopic molecule in acetonitrile solution shows depolarized Raman bands at 520, 420, and 310 $cm^{-1}$ as well as a polarized band at 335.3 $cm^{-1}$ (the region around 350 $cm^{-1}$ is obscured by the NCC deformation in free acetonitrile). In nitromethane solution, where the 350-$cm^{-1}$ region is not obscured by the solvent, the 335-$cm^{-1}$ band was observed but no feature was found at 358 $cm^{-1}$. Therefore, it appears that the 358-$cm^{-1}$ band found in the solid state shifts to 335 $cm^{-1}$ in solution and can be assigned to the symmetric mode $\nu_7$.

The two linear angle deformation modes $\nu_{14}$ and $\nu_{16}$ can be assigned to the bands at *ca.* 420 and *ca.* 100 $cm^{-1}$, respectively. The former assignment corresponds to an increase of *ca.* 40 $cm^{-1}$ from the NCC deformation mode in free acetonitrile.[14] (Our unpublished spectra of the boron trichloride and boron tribromide adducts of acetonitrile also exhibit a peak around 420 $cm^{-1}$ indicating that this peak is not associated with the $BF_3$ portion of the molecule.) The low-frequency assignment for $\nu_{16}$ is physically reasonable since the B–N bond is weak. While $\nu_{16}$ could be assigned to the bands at

(15) R. L. Amster and R. C. Taylor, *Spectrochim. Acta*, **20**, 1487 (1964).
(16) R. C. Taylor, H. S. Gabelnick, K. Aida, and R. L. Amster, *Inorg. Chem.*, **8**, 605 (1969).
(17) A. W. Laubengayer and D. S. Sears, *J. Am. Chem. Soc.*, **67**, 164 (1945).

*ca.* 130 or *ca.* 100 $cm^{-1}$, the band at *ca.* 130 $cm^{-1}$ was eliminated for three reasons: (1) the normal-coordinate analysis which was judged unreasonable for the higher frequency assignment, (2) the absence of a shift of this band for heavier boron halide adducts, and (3) the apparent 20-$cm^{-1}$ shift of the low-frequency band when chlorine is substituted for fluorine. The possibility that the 310-$cm^{-1}$ band is two nearly coincident fundamentals, one of which is $\nu_{16}$, was also considered but found unreasonable on the basis of a normal-coordinate treatment described in the next section.

The two remaining skeletal vibrations $\nu_{13}$ and $\nu_{15}$ can be assigned to the two remaining bands at *ca.* 310 and *ca.* 520 $cm^{-1}$. However, it is not clear which should be assigned to which fundamental. In both $F_3BNH_3$ and $F_3BN(CH_3)_3$ Taylor, *et al.*, assigned[15,16] the lower frequency to $BF_3$ deformation and the higher band to $BF_3$ rock. We prefer to assign the $BF_3$ deformation, $\nu_{13}$, in the acetonitrile adduct to the band at *ca.* 520 $cm^{-1}$ and the $BF_3$ rock $\nu_{15}$ to the band at *ca.* 310 $cm^{-1}$. This set of assignments is more reasonable for the present case because of the weak nature of the $BF_3$–acetonitrile bond. The $^{10}B$, $^{11}B$ and $^{14}N$, $^{15}N$ isotopic shifts do not help to distinguish between these two modes since insignificant isotope effects are noted for both bands.

The band found in the Raman spectra at *ca.* 130 $cm^{-1}$ could be a lattice mode. This interpretation cannot be checked by solution spectra since the region is obscured by the broad Rayleigh line.

In summary $\nu_7$ can be assigned unambiguously to the polarized band at 350 $cm^{-1}$ since it is the only symmetric mode expected in this region. The linear angle deformations, $\nu_{14}$ and $\nu_{16}$, can be assigned with relative certainty to the bands at *ca.* 420 and *ca.* 100 $cm^{-1}$. There is some uncertainty in the assignment of $\nu_{13}$ and $\nu_{15}$; however, the assignments given here are supported by the normal coordinate analysis.

**Unusual Temperature and Lattice Effects.**—Comparison of infrared spectra obtained at −196° (Figure 3) and −78° (Figure 4) shows that upon warming two very intense doublets appear at *ca.* 1505 and *ca.* 1455 $cm^{-1}$ while very sharp spikes appear at 1360, 718, 691, and 429 $cm^{-1}$. These features are probably dependent on lattice vibrations because they are not observed for the deuterated molecules or for 3% $^{10}B$ in host crystals of $^{10}BD$ (Figure 5).

The pair of high-frequency doublets have much larger integrated intensities than the lower frequency spikes. The latter features may originate from overtone or combination bands which appear at −78° because of motional narrowing, while they may be undetected at −196° due to large half-widths. The higher frequency doublets must involve a large increase in extinction coefficient at the higher temperature and must orginate from an increase in the transition moment integral, possibly through a change in the selection rules.

While we cannot detail the mechanism or assignments of the temperature-dependent bands, a number of known structural features may have bearing on them. On the nmr time scale,[18] it is known that the methyl group is reorienting down to the lowest temperature studied, −196°, and that the onset of the reorientation of the boron trifluoride group is around −143°. Similarly, X-ray diffraction results[13] indicate that the methyl group equally occupies eclipsed and staggered conformations relative to the boron trifluoride group, and the fluorine atoms show a great deal of thermal motion. This opens the possibility of a change in selection rules, providing that methyl reorientation occurs on the infrared time scale. Therefore, a permutation group treatment[19] was applied assuming that the hydrogens permute within both conformations while the rest of the molecule is constrained to the rigid $C_s$ site symmetry. The resulting permutation group is isomorphous with the point group $C_{6h}$ and selection rules were readily determined. The only important difference between the $C_{3v}$ symmetry and the permutation symmetry treatments is that the E symmetry $CH_3$ rock and stretch modes in the latter are active only in the infrared spectra. Thus, the temperature-dependent features cannot result from selection rule changes for a localized model involving methyl group reorientation. It is possible, however, that the methyl group reorientation causes an increase in the anharmonicity of the vibrations which in turn results in an increase in intensity of overtone and combination bands.[20]

### Calculation of Force Constants

Symmetry force constants were calculated using Schachtschneider's iterative least-squares program and associated programs.[21] The program minimizes the function $\Sigma[(\lambda_i)_{obsd} - (\lambda_i)_{calcd}]^2$; therefore, individual eigenvalues were weighted as $w_i = 1/\lambda_i$.[22] A local program COTRANS was used to calculate the valence force constants and their standard deviations from the symmetry force constants and the variance–covariance matrix.

In general there is good agreement between Raman and infrared frequencies so the latter were mainly used for refinement. Those fundamentals which were found to be split in the infrared spectra (see previous section) were included in the refinement after averaging the two peak positions. Treatment of data from the confusing region around 900 $cm^{-1}$, which contains $\nu_4$ (D molecules) and $\nu_5$, merits special comment. Raman and infrared positions for $\nu_5$ were quite different so these frequencies were averaged for use in the normal-coordinate treatment. No Raman data are available for the $^{15}N$ molecule, and the position of $\nu_5$ for the $^{10}BD$ molecule is uncertain; therefore $\nu_5$ for these two isotopic species was not included in the refinement. For the

(18) B. A. Donell, C. A. Fyfe, C. A. McDowell, and J. Ripmeester, *Trans. Faraday Soc.*, **65**, 1153 (1969).

(19) H. C. Longuet-Higgins, *Mol. Phys.*, **6**, 445 (1963).

(20) E. B. Wilson, J. C. Decius, and P. C. Cross, "Molecular Vibrations," McGraw-Hill Book Co., Inc., New York, N. Y., 1955, p 196.

(21) R. G. Snyder, and J. H. Schachtschneider, *Spectrochim. Acta*, **19**, 85 (1963); *cf.* GMAT and FPERT (locally modified) in J. H. Schachtschneider, "Vibrational Analysis of Polyatomic Molecules V and VI," Reports 231-64 and 57-65, Shell Development Co., Emeryville, Calif.

(22) A more reasonable weighting scheme would be $(\epsilon_i\lambda_i)^{-1}$ where $\epsilon_i$ is the estimated error in the eigenvalue $\lambda_i$. However, the errors are not well known so this procedure was not employed.

TABLE IV[a]

OBSERVED AND CALCULATED FUNDAMENTAL FREQUENCIES AND DIFFERENCES FOR FIVE ISOTOPIC VARIETIES OF $F_3BNCCH_3$ ($cm^{-1}$)

| | $^{11}B$ | | | $^{11}BD$ | | | $^{11}B^{15}N$ | | | $^{10}B$ | | | $^{10}BD$ | | |
|---|---|---|---|---|---|---|---|---|---|---|---|---|---|---|---|
| | Obsd | Calcd | Δ | Obsd | Calcd | Δ | Obsd | Calcd | Δ | Obsd | Calcd | Δ | Obsd | Calcd | Δ |
| $\nu_1(\nu_{C-H})$ | 2956 | 2954.0 | 2.0 | 2123.5 | 2127.5 | −4.0 | 2955.8 | 2954.0 | 1.9 | 2957.0[b] | 2954.0 | 3.0 | 2121.9 | 2127.5 | −5.6 |
| $\nu_2(\nu_{C-N})$ | 2376.2 | 2375.4 | 0.8 | 2373 | 2378.5 | −5.5 | 2338.4[c] | 2342.8 | 4.0 | 2373.9 | 2375.5 | −1.6 | 2373.8[b] | 2378.6 | −4.8 |
| $\nu_3(\delta_{CH_3})$ | 1372.0 | 1372.5 | −0.5 | 1106.7 | 1105.6 | 1.1 | 1373.3 | 1372.5 | 0.8 | 1374.2[b] | 1372.5 | 1.8 | 1106.6 | 1105.7 | 0.9 |
| $\nu_4(\nu_{C-C})$ | 978.7 | 979.2 | −0.5 | 892.2 | 890.4 | 1.8 | 968.7 | 968.3 | 0.4 | 979.0 | 980.4 | −1.4 | 899.8[b] | 900.4 | −0.6 |
| $\nu_5(\nu_{B-F})$ | 869.5 | 866.3 | 3.2 | 863.9 | 863.9 | 0.0 | 879.0[b] | 866.2 | 12.8 | 883.8 | 886.7 | −2.9 | 886.6[b] | 875.7 | 9.9 |
| $\nu_6(\nu_{B-N})$ | 651.4 | 650.4 | 1.0 | 647.5 | 646.6 | 3.4 | 654.6[b] | 650.4 | 4.2 | 660.5 | 663.3 | −1.7 | 655.9[b] | 658.2 | −2.3 |
| $\nu_7(\delta_{BF_3})$ | 359.2 | 361.3 | −2.1 | 348.7 | 349.9 | −1.2 | 356.1 | 359.6 | −3.5 | 358.6[b] | 361.4 | 2.8 | 347.8 | 350.1 | −2.3 |
| $\nu_8(\nu_{C-H})$ | 3029.5 | 3028.7 | 0.8 | 2271 | 2268.7 | 2.3 | 3026 | 3028.7 | −2.7 | 3029[b] | 3028.7 | 0.8 | 2269 | 2268.7 | 0.3 |
| $\nu_{10}(\delta_{CH_3})$ | 1430 | 1433.0 | −3.0 | 1024.7 | 1023.4 | 1.3 | 1420[b] | 1433.0 | −13.0 | 1430[b] | 1433.0 | −3.0 | 1025.7 | 1023.4 | 2.3 |
| $\nu_{11}(\nu_{B-F})$ | 1170[b] | 1164.9 | 5.1 | 1170 | 1164.3 | 5.1 | 1170[b] | 1164.9 | −5.1 | 1205.8 | 1211.0 | −5.2 | 1206 | 1211.0 | −5.0 |
| $\nu_{12}(\rho_{CH_3})$ | 1031.4 | 1032.8 | −1.4 | 848 | 844.9 | 3.1 | 1032 | 1032.5 | −0.5 | 1028.6[b] | 1032.8 | −4.2 | 850 | 844.9 | 5.1 |
| $\nu_{13}(\delta_{BF_3})$ | 520.9 | 525.9 | −5.0 | 518.8 | 515.9 | 0.9 | 516.0 | 519.1 | −3.1 | 522.0[b] | 526.5 | −4.5 | 518.7 | 516.7 | 2.0 |
| $\nu_{14}(\delta_{NCC})$ | 422.8 | 423.7 | −0.9 | 407 | 406.8 | 0.2 | 417.7 | 422.3 | −4.6 | 422.2[b] | 424.0 | −1.8 | 406.5 | 406.9 | −0.4 |
| $\nu_{15}(\rho_{BF_3})$ | 314.3 | 308.9 | 5.4 | 298.6 | 297.8 | 0.8 | 312.8 | 308.9 | 4.8 | 313.9[b] | 309.2 | 4.7 | 298.1 | 298.0 | 0.1 |
| $\nu_{16}(\delta_{BNC})$ | 98.5 | 103.1 | −4.6 | 97.3 | 98.1 | −0.8 | ...[b] | 102.1 | ... | 100.1[b] | 103.1 | −3.1 | 98.0 | 98.1 | −0.1 |

[a] $A_1$ class: average deviation 2.4 $cm^{-1}$; E class: average deviation 2.8 $cm^{-1}$ for frequencies used in refinement; $\Delta = \nu(\text{exptl}) - \nu(\text{calcd})$. [b] Frequency not included in refinement. [c] Position corrected for Fermi resonance with $\nu_3 + \nu_4$.

TABLE V

MOLECULAR PARAMETERS AND COORDINATES FOR $F_3BNCCH_3$

| Bond lengths, Å | Bond angles, deg |
|---|---|
| $r$ = C—H = 1.157 | $\alpha$ = HCH = 109.52 |
| $R$ = B—F = 1.347 | $\beta$ = CCH = 109.52 |
| $d$ = B—N = 1.630 | $\delta$ = FBF = 113.13 |
| $D$ = C≡N = 1.135 | $\gamma$ = NBF = 105.50 |
| $L$ = C—C = 1.439 | $\rho$ = BNC = 180.00 |
| | $\epsilon$ = NCC = 180.00 |

Symmetry Coordinates[a,b]

$A_1$ Class

$$S_1 = (1/\sqrt{3})(\Delta r_1 + \Delta r_2 + \Delta r_3)$$
$$S_2 = \Delta D$$
$$S_3 = (1/\sqrt{n_1})[m_1(\Delta\alpha_1 + \Delta\alpha_2 + \Delta\alpha_3) - (\Delta\beta_1 + \Delta\beta_2 + \Delta\beta_3)]$$
$$S_4 = \Delta L$$
$$S_5 = (1/\sqrt{3})(\Delta R_1 + \Delta R_2 + \Delta R_3)$$
$$S_6 = \Delta d$$
$$S_7 = (1/\sqrt{n_2})[m_2(\Delta\gamma_1 + \Delta\gamma_2 + \Delta\gamma_3) - (\Delta\delta_1 + \Delta\delta_2 + \Delta\delta_3)]$$

E Class

$$S_9 = (1/\sqrt{2})(\Delta r_2 - \Delta r_3)$$
$$S_{10} = (1/\sqrt{2})(\Delta\alpha_2 - \Delta\alpha_3)$$
$$S_{11} = (1/\sqrt{2})(\Delta R_2 - \Delta R_3)$$
$$S_{12} = (1/\sqrt{2})(\Delta\beta_2 - \Delta\beta_3)$$
$$S_{13} = (1/\sqrt{2})(\Delta\delta_2 - \Delta\delta_3)$$
$$S_{14} = \Delta\epsilon$$
$$S_{15} = (1/\sqrt{2})(\Delta\gamma_2 - \Delta\gamma_3)$$
$$S_{16} = \Delta\rho_1$$

[a] The molecule is in a staggered conformation. The projections of $R_1$ and $r_1$ along the threefold axis make an angle of 180° with each other. The angle $\alpha_1$ lies between $r_2$ and $r_3$, etc. [b] $m_1 = -\sqrt{3}\cos\beta/\cos(\alpha/2)$, $n_1 = 3(m_1^2 + 1)$, $m_2 = -\sqrt{3}\cos\gamma/\cos(\delta/2)$, $n_2 = 3(m_2^2 + 1)$.

deuterated molecules, $\nu_4$ is taken from the Raman data since it is obscured by $\nu_5$ in the infrared spectra. The infrared and Raman vibrational data at *ca.* 650 $cm^{-1}$ for $\nu_6$ also were averaged. The frequencies are uncertain for $\nu_{11}$ of the normal and $^{15}N$ isotopic molecules and for $\nu_{16}$ of the $^{15}N$ molecule so these were not included in the refinement. Table IV summarizes all of the frequencies employed in the refinement.

The molecular parameters used in the calculation of the $G$ matrix elements were obtained from two sources. Bond lengths and angles involving heavy atoms were taken from the crystal structure.[13] Since the molecule was assumed to possess $C_{3v}$ symmetry, the bond lengths and angles related by symmetry were averaged. The methyl group was assumed to be tetrahedral and the C–H bond length was taken from that found in acetonitrile.[23] The bond parameters and symmetry coordinates are presented in Table V. Since the vibrational problem is underdetermined, constraints need to be applied to the force field. The general constraint applied to both symmetry blocks was to neglect stretch–stretch interaction constants between symmetry coordinates which do not have a common atom and stretch–bend, bend–bend interaction constants between symmetry coordinates which do not have a common bond.

For the acetonitrile part of the molecule the initial constants were taken from Duncan's calculation.[24] The two E symmetry block interaction constants $F_{12,14}$ and $F_{9,10}$ were fixed at Duncan's values since they are accurately determined in free acetonitrile by Coriolis data. These two constants are not expected to change upon adduct formation since they involve symmetry coordinates localized on the methyl portion of the molecule. In the final refinement two $A_1$ and two E interaction constants were refined simultaneously for the acetonitrile part of the molecule.

For the $BF_3$ part of the molecule five interaction constants in the $A_1$ symmetry block[25] and five interaction constants in the E block were included. The initial constants for the acid portion of the molecule were taken from Clippard's force field for $F_3BN(CH_3)_3$[26] and modified using the Jacobian matrix before refinement was begun. Only three interaction constants could be

(23) C. C. Costain, *J. Chem. Phys.*, **29**, 864 (1958).

(24) J. L. Duncan, *Spectrochim. Acta*, **20**, 1197 (1964). The interaction constant $F_{2,4}$ appears to be dependent on the phase of the acetonitrile. The value of 0.0 was taken from our analysis of liquid-phase data for $NCCH_3$, $^{15}NCCH_3$, and $NCCD_3$.

(25) Interaction constants $F_{4,6}$ (BN and CC stretch) and $F_{2,6}$ (C≡N and BN stretch) were also included in the treatment since the Jacobian matrix showed that these constants affected $\nu_2$, $\nu_4$, and $\nu_6$. The values for these two constrained constants were obtained by changing each one so as to minimize approximately correlation of the force constants and obtain a reasonable PED while maintaining good agreement between observed and calculated frequencies. The C≡N force constant, $F_{22}$, is relatively insensitive to changes in these force constants; however, the BN force constant, $F_{66}$, is sensitive to these force constants as well as the BF–BN interaction constant, $F_{56}$. Variation of these interaction constants by factors of 20–80% will give a poorer but acceptable fit to the data. Under these conditions $F_{66}$ varies by ±9%.

(26) P. D. H. Clippard, Doctoral Thesis, University of Michigan, 1969.

TABLE VI

POTENTIAL ENERGY DISTRIBUTION FOR $F_3BNCCH_3$, E CLASS

| | $\nu_9$ = 3029 cm$^{-1}$ | $\nu_{10}$ = 1430 cm$^{-1}$ | $\nu_{11}$ = 1170 cm$^{-1}$ | $\nu_{12}$ = 1031 cm$^{-1}$ | $\nu_{13}$ = 521 cm$^{-1}$ | $\nu_{14}$ = 423 cm$^{-1}$ | $\nu_{15}$ = 314 cm$^{-1}$ | $\nu_{16}$ = 99 cm$^{-1}$ |
|---|---|---|---|---|---|---|---|---|
| $V_{9,9}$[a] | 0.96 | 0.06 | 0.0 | 0.0 | 0.0 | 0.0 | 0.0 | 0.0 |
| $V_{10,10}$ | 0.01 | 0.91 | 0.0 | 0.10 | 0.0 | 0.0 | 0.0 | 0.0 |
| $V_{11,11}$ | 0.0 | 0.0 | 0.79 | 0.0 | 0.11 | 0.16 | 0.09 | 0.01 |
| $V_{12,12}$ | 0.0 | 0.09 | 0.0 | 0.79 | 0.04 | 0.07 | 0.03 | 0.01 |
| $V_{13,13}$ | 0.0 | 0.0 | 0.24 | 0.0 | 0.12 | 0.41 | 0.25 | 0.0 |
| $V_{14,14}$ | 0.0 | 0.0 | 0.0 | 0.06 | 0.21 | 0.44 | 0.27 | 0.07 |
| $V_{15,15}$ | 0.0 | 0.0 | 0.09 | 0.0 | 0.28 | 0.02 | 0.70 | 0.11 |
| $V_{16,16}$ | 0.0 | 0.0 | 0.01 | 0.0 | 0.14 | 0.10 | 0.0 | 0.76 |
| $V_{9,10}$ | 0.03 | −0.07 | 0.0 | 0.01 | 0.0 | 0.0 | 0.0 | 0.0 |
| $V_{9,12}$ | 0.0 | −0.01 | 0.0 | 0.01 | 0.0 | 0.0 | 0.0 | 0.0 |
| $V_{10,12}$ | 0.0 | 0.02 | 0.0 | −0.02 | 0.0 | 0.0 | 0.0 | 0.0 |
| $V_{11,13}$ | 0.0 | 0.0 | 0.02 | 0.0 | −0.01 | −0.01 | −0.01 | 0.0 |
| $V_{11,15}$ | 0.0 | 0.0 | −0.19 | 0.0 | 0.12 | −0.04 | −0.19 | −0.03 |
| $V_{12,14}$ | 0.0 | 0.0 | 0.0 | 0.07 | −0.03 | −0.06 | −0.03 | −0.01 |
| $V_{13,15}$ | 0.0 | 0.0 | 0.04 | 0.0 | 0.06 | −0.03 | −0.12 | 0.0 |
| $V_{14,16}$ | 0.0 | 0.0 | 0.0 | −0.01 | −0.06 | −0.08 | 0.01 | 0.08 |
| $V_{15,16}$ | 0.0 | 0.0 | 0.0 | 0.0 | 0.0 | 0.0 | 0.0 | 0.01 |

[a] The subscripts identify $V_{kl}$ with symmetry coordinates $k$ and $l$ as defined in Table V.

refined simultaneously with the diagonal constants in the $A_1$ block. If four interaction constants were refined, the normal equation could not be solved due to a singularity in the inversion of **B**.[27] A close examination of the correlation coefficients indicated that the four interaction or diagonal constants were not highly correlated. Since the constants included in the refinement are reasonably independent, then the singularity must arise from an insufficient number of independent frequencies. The frequencies from the four isotopic molecules for the $BF_3$ related modes far outnumber the force constants included in the refinement. However, the lack of independence in these four sets of frequencies is reasonable since none of the $BF_3$ vibrations is greatly influenced by isotopic substitution.

The same problem exists for the E block, so only four interaction constants ($F_{9,12}$, $F_{10,12}$, $F_{13,15}$, and $F_{15,16}$) could be refined simultaneously with the diagonal constants, and the remaining interaction constants were constrained.[28]

The potential energy distribution shows that the low-frequency modes are highly mixed, and the band at *ca.* 520 cm$^{-1}$ cannot be attributed to any particular vibration (Table VI). The predominant contributors in each of the remaining normal modes are in agreement with the proposed assignments. The potential energy distribution for the $A_1$ block is presented in Table VII and the final symmetry force constants are given in Table VIII. The final fit between observed and calculated frequencies is presented in Table IV.

To check the very low assigned frequency for the BNC deformation, attempts were made to adjust $\nu_{16}$ (E, BNC deformation) to the *ca.* 310-cm$^{-1}$ band and also to the *ca.* 130-cm$^{-1}$ band (see previous section). About 195 cm$^{-1}$ was the highest value which could be obtained for the low-frequency mode in the E block without introducing excessive errors in the other frequencies. For this solution the primary force constants for NCC and BNC deformations were unrealistically high: $F_{NCC} \approx 0.6$ and $F_{BNC} \approx 0.8$, *vs.* $F_{NCC} \approx 0.4$ for free acetonitrile. A force field was found using the 130-cm$^{-1}$ assignment for $\nu_{16}$, which resulted in good agreement between observed and calculated frequencies. However, the PED showed that the low-frequency modes, 423 and 314 cm$^{-1}$, were highly mixed and the predominant contributor in these modes did not correspond to the proposed assignments. For example, the 423-cm$^{-1}$ band had a primary contribution from $CH_3$ deformation with NCC and NBF deformations contributing only slightly less. In addition, the values for the primary force constants for the two linear angle deformation modes were again unrealistically high ($F_{NCC} = 0.64$, $F_{BNC} = 0.43$). Therefore, the original assignment of $\nu_{16}$ is preferred.

TABLE VII

POTENTIAL ENERGY DISTRIBUTION FOR $F_3{}^{11}BNCCH_3$, $A_1$ CLASS

| | $\nu_1$ = 2954 cm$^{-1}$ | $\nu_2$ = 2375 cm$^{-1}$ | $\nu_3$ = 1372 cm$^{-1}$ | $\nu_4$ = 979 cm$^{-1}$ | $\nu_5$ = 866 cm$^{-1}$ | $\nu_6$ = 650 cm$^{-1}$ | $\nu_7$ = 361 cm$^{-1}$ |
|---|---|---|---|---|---|---|---|
| $V_{11}$[a] | 0.99 | 0.0 | 0.0 | 0.0 | 0.0 | 0.0 | 0.0 |
| $V_{22}$ | 0.0 | 0.87 | 0.0 | 0.05 | 0.0 | 0.02 | 0.06 |
| $V_{33}$ | 0.0 | 0.0 | 1.04 | 0.0 | 0.0 | 0.0 | 0.0 |
| $V_{44}$ | 0.0 | 0.10 | 0.08 | 0.79 | 0.0 | 0.02 | 0.05 |
| $V_{55}$ | 0.0 | 0.0 | 0.0 | 0.0 | 1.00 | 0.10 | 0.0 |
| $V_{66}$ | 0.0 | 0.02 | 0.0 | 0.17 | 0.22 | 0.39 | 0.48 |
| $V_{77}$ | 0.0 | 0.0 | 0.0 | 0.01 | 0.35 | 0.74 | 0.17 |
| $V_{13}$ | 0.0 | 0.0 | 0.0 | 0.0 | 0.0 | 0.0 | 0.0 |
| $V_{14}$ | 0.0 | 0.0 | 0.0 | 0.0 | 0.0 | 0.0 | 0.0 |
| $V_{24}$ | 0.0 | 0.0 | 0.0 | 0.0 | 0.0 | 0.0 | 0.0 |
| $V_{26}$ | 0.0 | 0.01 | 0.0 | 0.01 | 0.0 | −0.01 | −0.01 |
| $V_{34}$ | 0.0 | 0.0 | −0.13 | 0.02 | 0.0 | 0.0 | 0.0 |
| $V_{46}$ | 0.0 | 0.0 | 0.0 | −0.02 | 0.0 | 0.01 | 0.01 |
| $V_{56}$ | 0.0 | 0.0 | 0.0 | −0.01 | −0.17 | 0.07 | −0.01 |
| $V_{57}$ | 0.0 | 0.0 | 0.0 | 0.0 | −0.18 | 0.08 | 0.01 |
| $V_{67}$ | 0.0 | 0.0 | 0.0 | −0.03 | −0.22 | −0.43 | 0.23 |

[a] See footnote *a*, Table VI.

(27) **B** is the matrix of the normal equations in the least-squares analysis; see W. C. Hamilton, "Statistics in Physical Science," Ronald Press, New York, N. Y., 1964, p 127.

(28) The values for the constrained constants, $F_{11,13}$, $F_{11,15}$, and $F_{14,16}$, were obtained by changing each one so as to minimize approximately correlation of the force constants and obtain a reasonable PED while maintaining good agreement between observed and calculated frequencies. The diagonal constants which are most sensitive to the specific values of these off-diagonal **F** elements are $F_{11,11}$, $F_{14,14}$, and $F_{16,16}$.

TABLE VIII[a]

SYMMETRY FORCE CONSTANTS FOR $F_3BNCCH_3$

$A_1$ Class

| | | | | | |
|---|---|---|---|---|---|
| $F_{11}$ | 5.04 (2)[b] | $F_{66}$ | 2.54 (27) | $F_{26}$ | −0.25[c] |
| $F_{22}$ | 18.86 (4) | $F_{77}$ | 1.25 (14) | $F_{34}$ | −0.38 (2) |
| $F_{33}$ | 0.585 (4) | $F_{13}$ | 0.06 (6) | $F_{46}$ | 0.1[c] |
| $F_{44}$ | 5.32 (12) | $F_{14}$ | 0.0[c] | $F_{56}$ | 0.74 (44) |
| $F_{55}$ | 6.49 (36) | $F_{24}$ | 0.0[c] | $F_{57}$ | 0.44 (25) |
| | | | | $F_{67}$ | −0.72 (7) |

E Class

| | | | | | |
|---|---|---|---|---|---|
| $F_{99}$ | 4.78 (4) | $F_{15,15}$ | 1.00 (4) | $F_{11,15}$ | 0.71[c] |
| $F_{10,10}$ | 0.55 (2) | $F_{16,16}$ | 0.20 (1) | $F_{12,14}$ | −0.09[c] |
| $F_{11,11}$ | 3.76 (17) | $F_{9,10}$ | 0.09[c] | $F_{13,15}$ | −0.16 (5) |
| $F_{12,12}$ | 0.62 (3) | $F_{9,12}$ | 0.24 (6) | $F_{14,16}$ | 0.05[c] |
| $F_{13,13}$ | 1.14 (13) | $F_{10,12}$ | 0.02 (4) | $F_{15,16}$ | −0.01 (3) |
| $F_{14,14}$ | 0.45 (3) | $F_{11,13}$ | 0.05[c] | | |

[a] The subscripts identify $F_{kl}$ with symmetry coordinates $k$ and $l$ as defined in Table V. Force constants $F_{33}$, $F_{77}$, $F_{10,10}$, $F_{12,12}$, $F_{13,13}$, $F_{14,14}$, $F_{15,15}$, $F_{16,16}$, $F_{10,12}$, $F_{12,14}$, $F_{13,15}$, $F_{14,16}$, and $F_{15,16}$ are in units of mdyn Å/(radian)$^2$ while constants $F_{13}$, $F_{23}$, $F_{34}$, $F_{57}$, $F_{67}$, $F_{9,10}$, $F_{9,12}$, $F_{11,13}$, and $F_{11,15}$ are in units of mdyn/radian. The remainder are in units of mdyn/Å. [b] Least-squares standard deviations are given in parentheses. [c] Force constant constrained.

## Discussion

A complete set of assignments for the fundamental vibrations of acetonitrile–boron trifluoride has been obtained for the first time (Tables II and III). In previous work, Le Calvé has reported frequencies for the $BF_3$ portion of this molecule.[4] These data, which were obtained at −196°, are in good agreement with our observations. However, we differ in assignments for the low-frequency region. Vibrations of $A_1$ symmetry for the acetonitrile portion of $CH_3CNBF_3$ were reported by Purcell and Drago.[5] Their frequencies, which were obtained at room temperature, are consistently 10–15 cm$^{-1}$ lower than ours. Finally, Coerver and Curran[3] observed a C≡N stretching frequency which is lower than our value but within the accuracy of their instrumentation. Some of the foregoing disparities may originate from temperature differences or decomposition of the adduct through reaction with alkali halide window materials or pellets because, with the exception of Le Calvé, previous workers have overlooked this mode of decomposition. Also no isotopic data have been reported previously.

With the exception of CC and C≡N stretching frequencies, the fundamentals associated with the acetonitrile portion of $F_3BNCCH_3$ are similar to those of free acetonitrile. The usual increase in C≡N stretching frequency upon coordination is found for $F_3BNCCH_3$.[29] Also, a surprising increase of *ca.* 60 cm$^{-1}$ is found for the CC stretch.

Interesting trends are found by comparing $BF_3$ and BN stretching frequencies between adducts of $BF_3$ with various Lewis bases (Table IX). The B-donor stretching frequency drops *ca.* 100 cm$^{-1}$ on going from the relatively strong Lewis base $NH_3$ to the weaker base $NCCH_3$. In line with previous observations,[4] the separation between symmetric and antisymmetric $BF_3$ stretch increases on going from a strong to a weak base.

(29) R. A. Walton, *Quart. Rev.* (London), **19**, 126 (1965).

TABLE IX

COMPARISON OF VIBRATIONAL FREQUENCIES (CM$^{-1}$) FOR $^{11}BF_3$ ADDUCTS

| | Donor molecule | | | | |
|---|---|---|---|---|---|
| | $NH_3$[a] | $N(CH_3)_3$[b] | $NCCH_3$ | $(CH_3)_2O$[c] | $(CH_3)_2S$[c] |
| $\nu_{a,BF_3}$ str | 1146 | 1144 | 1170 | 1200 | 1160 |
| $\nu_{s,BF_3}$ str | 991 | 929 | 870 | 850 | 835 |
| $\nu_{s,B\text{-donor}}$ str | 742 | 694 | 651 | 660 | 628 |
| $\delta_{s,BF_3}$ def | 518 | 330 | 358 | 390 | 340 |
| $\delta_{a,BF_3}$ def | 334 | 323 | 521 | 505 | 469 |
| $\rho_{a,BF_3}$ rock | 476 | 520 | 314 | ? | ? |

[a] From ref 16. [b] From ref 26. [c] $(CH_3)_2O$ data for liquid state and $(CH_3)_2S$ data for solid state; see ref 4.

In $F_3BNH_3$ this separation is only *ca.* 155 cm$^{-1}$ while in $F_3BNCCH_3$ it is *ca.* 300 cm$^{-1}$. Comparisons of enthalpies[30] of formation of $F_3BNH_3$, $F_3BN(CH_3)_3$, and $F_3BNCCH_3$ with either $\nu_{BN}$ or the separation between symmetric and antisymmetric $BF_3$ stretch show that as the enthalpy becomes more negative, $\nu_{BN}$ and $(\nu_{asym,BF_3} - \nu_{sym,BF_3})$ increase. In addition, a plot of $\nu_{BN}$ *vs.* $(\nu_{asym,BF_3} - \nu_{sym,BF_3})$ for these three adducts is linear. Both the BN stretching frequency and the separation between symmetric and antisymmetric $BF_3$ stretching frequency appear to be quite sensitive to the strength of the Lewis base and therefore the strength of the donor adduct bond.

To our knowledge, this is the first time Raman polarization data have been obtained for the low-frequency vibrations of a $BF_3$ adduct with $C_{3v}$ symmetry. These data provide a definite assignment for the symmetric $BF_3$ deformation which is found at *ca.* 350 cm$^{-1}$. If existing assignments for other $BF_3$ adducts are accepted, there are no simple trends for $BF_3$ skeletal vibrations (Table IX). However, this may be due to difficulties in making assignments for the low-frequency region. Another possible reason for the lack of trends may be the lack of purity of the low-frequency vibrations.

The potential energy distribution, $V_{kl,\nu_i} = L_{k,\nu_i} \cdot F_{kl} L_{l,\nu_i}$, obtained from the normal-coordinate analysis, shows that many of the lower frequency vibrations involve substantial contributions from more than one symmetry coordinate. In the $A_1$ symmetry class the three low-frequency modes show contributions from BN and $BF_3$ stretch and from $BF_3$ deformation (Table VII). The BN stretch force constant also contributes substantially to the CC stretching mode. It is impossible, therefore, to characterize these low-frequency modes as distinct vibrations.

In the E symmetry block, the modes above 600 cm$^{-1}$ ($BF_3$ stretch and the acetonitrile frequencies with the exception of NCC deformation) are relatively pure. The low-frequency modes are highly mixed; however, the PED supports the proposed assignments.

The increase in the C≡N stretching frequency upon coordination to Lewis acids is observed for virtually all nitriles.[29] In acetonitrile this increase has been attributed in part to a substantial increase in the C≡N stretching force constant.[5,6] A comparison of the pri-

(30) (a) $F_3BNH_3$, A. W. Laubengayer and G. F. Clondike, *J. Am. Chem. Soc.*, **70**, 2274 (1948); (b) $F_3BN(CH_3)_3$, A. Shepp and S. H. Bauer, *ibid.*, **76**, 265 (1954); (c) $F_3BNCCH_3$, ref 17.

mary C≡N stretching force constants for the $BF_3$ adduct ($f_{CN}$ = 18.8 mdyn/Å) with that of the free acetonitrile[31] ($f_{CN}$ = 17.4 mdyn/Å) shows that this constant does increase upon adduct formation. The increase in $f_{CN}$ indicates an increase in the C≡N bond strength upon coordination, which agrees with the decrease in the C≡N bond length observed in the crystal structures.[13]

The CC stretching frequency is also found to increase upon adduct formation and there is an indication that the bond length may decrease. However, the force constants for the adduct ($f_{CC}$ = 5.32 mdyn/Å) and for free acetonitrile ($f_{CC}$ = 5.3 mdyn/Å) agree within their limits of error. Part of the increase in $\nu_4$ can be attributed to kinematic coupling with BN stretch since this force constant contributes to the CC stretching frequency. The increase in $F_{11}$ and $F_{99}$ and the decrease in $F_{33}$ and $F_{10,10}$ agree with the shifts observed for $\nu_1$, $\nu_3$, $\nu_9$, and $\nu_{10}$ upon complexation. The remaining force constants for the acetonitrile part of the molecule are similar to those of free acetonitrile.

(31) The CN force constant of free acetonitrile used here was determined from liquid vibrational data on $H_3CC^{15}N$, $H_3CCN$, and $D_3CCN$. Comparisons with this force field minimize the errors resulting from phase differences, since the frequencies for nitriles are known to be phase dependent: B. H. Thomas and W. L. Orville-Thomas, *J. Mol. Struct.*, **3**, 161 (1969). In this force field, $f_{CN}$ is lower than that of Duncan[24] and the difference may be attributed to the phase dependence of $\nu_{CN}$ and the change in the off-diagonal constant involving C≡N and CC bond stretch interaction.

The force constant for the donor–acceptor BN bond is of particular interest. The BN valence force constants for $F_3BNH_3$, $F_3BN(CH_3)_3$, and $F_3BNCCH_3$ are 3.97,[16] 3.53,[26] and 2.5 mdyn/Å. Thus the decrease in $\nu_{BN}$ on going from a strong to a weak adduct is matched by a decrease in $f_{BN}$. The weak nature of the BN bond in $F_3BNCCH_3$ is clear from $\nu_{BN}$, $f_{BN}$, and the BN bond length ($r_{BN}$ = 1.63 Å).[13] However, a monotonic correlation is not found between $\nu_{BN}$, $f_{BN}$, or $\Delta H_f°$ and the BN bond lengths ($r_{BN}$ = 1.60 Å for $F_3BNH_3$ and $r_{BN}$ = 1.585 Å for $F_3BN(CH_3)_3$).[32]

The $BF_3$ stretching force constant shows the expected decrease upon coordination ($f_{BF}$ = 4.8 mdyn/Å for $F_3BNCCH_3$). However, no simple monotonic correlations involving $f_{BF}$ for adducts of this type can be found with the existing data.

**Acknowledgments.**—This research was supported by the National Science Foundation through Grants GP-6676 and -10117 and by the ARPA through the Northwestern Materials Research Center. We thank Professor R. C. Taylor for supplying a copy of P. Clippard's thesis and for helpful discussions. We are also grateful to Dr. G. M. Begun for a copy of Jacques Le Calve's thesis.

(32) J. L. Hoard, S. Geller, and T. B. Owen, *Acta Cryst.*, **4**, 405 (1951).

---

CONTRIBUTION FROM THE DEPARTMENT OF CHEMISTRY, UNIVERSITY OF KENTUCKY, LEXINGTON, KENTUCKY, AND THE U. S. ARMY RESEARCH OFFICE, DURHAM, NORTH CAROLINA

# Boron–Nitrogen Compounds. XXXIII.[1] A Normal-Coordinate Analysis of Borazine

BY KENNETH E. BLICK, JOHN W. DAWSON, AND KURT NIEDENZU

*Received December 1, 1969*

Utilizing a recent reassignment of the vibrational spectrum of borazine, $(-BH-NH-)_3$, and isotopically labeled derivatives thereof, a normal-coordinate analysis on this six-membered heterocycle has been performed. The calculated valence force field was adjusted to provide a good fit for all of the available data. When the entire set of suggested assignments for the normal vibrations of $(-BH-NH-)_3$, $(-^{10}BH-NH-)_3$, $(-BH-ND-)_3$, $(-^{10}BH-ND-)_3$, $(-BD-NH-)_3$, $(-^{10}BD-NH-)_3$, and $(-BD-ND-)_3$ was utilized in a simultaneous least-squares adjustment, the average error between all of the calculated and observed frequencies was 1.01%. The calculated force constants are in agreement with recent judgments on the strength of the various bonds in the borazine molecule. The calculated potential energy distribution of the isotopically labeled derivatives indicates that the character of several BH and NH vibrations is altered substantially upon deuteration at either the boron or the nitrogen atoms. Displacements calculated for the parent borazine molecule reveal appreciable movement of the annular atoms out of the molecular plane.

## Introduction

The vibrational spectrum of borazine, $(-BH-NH-)_3$, has been recently reexamined using isotopically labeled derivatives.[2] Based on the resultant data, reassignments of several fundamentals of borazine were suggested; they should have a significant bearing on the previously reported values[3-5] of a number of valence force constants of borazine. For example, a significant change in the B–N force constant was anticipated due to the reassignment of the highest B–N stretching mode of species E′ from 1605 to 1465 $cm^{-1}$.[2]

Also, some minor uncertainties had remained with respect to the assignment of fundamentals[2] and it

(1) Part XXXII: K. Niedenzu, P. J. Busse, and C. D. Miller, *Inorg. Chem.*, **9**, 977 (1970).

(2) K. Niedenzu, W. Sawodny, H. Watanabe, J. W. Dawson, T. Totani, and W. Weber, *ibid.*, **6**, 1453 (1967).

(3) B. L. Crawford and J. T. Edsall, *J. Chem. Phys.*, **7**, 233 (1939).

(4) R. A. Spurr and S. Chang, *ibid.*, **19**, 518 (1951).

(5) E. Silberman, *Spectrochim. Acta*, **23**, 2021 (1967).